INFLUENCE OF ROUGHNESS ON HEAT TRANSFER AND TRANSITION: ART PROGRAM DATA REPORT

R. E. Phinney, et al

Naval Ordnance Laboratory
White Oak, Maryland

19 December 1974

UNCLASSIFIED

SECURITY CLASSIFICATION OF THIS PAGE (When Data Entered)

AD 777384

REPORT DOCUMENTATION PAGE

READ INSTRUCTIONS BEFORE COMPLETING FORM

1. REPORT NUMBER: NOLTR 73-231	2. GOVT ACCESSION NO.
3. RECIPIENT'S CATALOG NUMBER	
4. TITLE (and Subtitle): Influence of Roughness on Heat Transfer and Transition; ART Program Data Report	5. TYPE OF REPORT & PERIOD COVERED
6. PERFORMING ORG. REPORT NUMBER: NOLTR 73-231	
7. AUTHOR(s): R. E. Phinney, F. P. Baltakis	8. CONTRACT OR GRANT NUMBER(s)
9. PERFORMING ORGANIZATION NAME AND ADDRESS: Naval Ordnance Laboratory, White Oak, Silver, Spring, Maryland 20910	10. PROGRAM ELEMENT, PROJECT, TASK AREA & WORK UNIT NUMBERS: NAVORD UF-323-22505
11. CONTROLLING OFFICE NAME AND ADDRESS: Naval Ordnance Systems Command, Washington, D. C. 20360	12. REPORT DATE: 15 December 1973
	13. NUMBER OF PAGES: 21
14. MONITORING AGENCY NAME & ADDRESS (if different from Controlling Office)	15. SECURITY CLASS. (of this report): UNCLASSIFIED
	15a. DECLASSIFICATION/DOWNGRADING SCHEDULE

16. DISTRIBUTION STATEMENT (of this Report)

Approved for public release; distribution unlimited.

17. DISTRIBUTION STATEMENT (of the abstract entered in Block 20, if different from Report)

18. SUPPLEMENTARY NOTES

19. KEY WORDS (Continue on reverse side if necessary and identify by block number)

Heat Transfer; Transition; Roughness

20. ABSTRACT (Continue on reverse side if necessary and identify by block number)

In order to assess the direct influence of surface roughness upon heat transfer and its indirect effect through the shift in transition location, a series of wind tunnel tests were carried out. A fixed body shape (with one exception) with varying roughness was tested at a series of tunnel conditions and the heat transfer measured by the thin wall calorimeter method. The wind tunnel conditions and the heat transfer distribution around the models are presented in tabular form.

DD FORM 1 JAN 73 1473 EDITION OF 1 NOV 65 IS OBSOLETE
S/N 0102-014-6601

UNCLASSIFIED

SECURITY CLASSIFICATION OF THIS PAGE (When Data Entered)

NOLTR 73-231 - 15 December 1973

INFLUENCE OF ROUGHNESS ON HEAT TRANSFER AND TRANSITION: ART PROGRAM DATA REPORT

This report summarizes the heat transfer rate data obtained in the NOL Hypersonic Tunnel under the Navy's Advanced Re-entry Technology (ART) program. The study was funded by the Naval Ordnance Systems Command, Washington, D. C., under the Task Number UF-323-22505.

ROBERT WILLIAMSON II
Captain, USN
Commander

Leon H. Schindel

LEON H. SCHINDEL
By direction

CONTENTS

	Page
INTRODUCTION	1
TEST APPARATUS	2
Test Conditions	2
Model Geometry and Instrumentation	2
Test Procedure	2
DATA REDUCTION AND PRESENTATION	3
Form of the Available Data	3
Treatment of the Data	3
Curve Fitting the Time-Temperature Data	4
Data Derived From the Fitted Curve	5
SYMBOLS	6

ILLUSTRATIONS

Figure	Title
1	NOL Hypersonic Tunnel
2	Model Geometry and Instrumentation Layout A. Sphere-Cone Configuration B. Blunted-Cone Configuration
3	Model Photograph A. Sphere-Cone With 80-Mil Roughness (Model No. 8) B. Blunted-Cone with 3-Mil Roughness (Model No. 9)
4	Samples of Temperature-Time Traces

TABLES

Table	Title
1	Test Conditions and Stagnation Point Initial Heating Rate
2	Model Wall to Stagnation Point Initial Heating Rate

REFERENCES

1. Baltakis, F. P., "Performance Capability of the NOL Hypersonic Tunnel", NOLTR 68-187, Oct 1968

INTRODUCTION

The present tests were conducted under the Navy's Advanced Reentry Technology (ART) program. The program is an extension of a test series conducted for the Air Force at the Naval Ordnance Laboratory (NOL) under the Passive Nosetip Technology (PANT) program. The primary concern of both programs is to improve the understanding of the effect of roughness on nosetip heat transfer, both directly and also indirectly through its influence upon transition.

Basically the work that was performed was the measurement of heat-transfer rate on thin-walled sphere-cone calorimeter models. A succession of seven models was run in the Hypersonic Tunnel at NOL. Each had an identical 2.5-inch nose radius and a 8° conical skirt but with successive models having a different surface roughness height in the range of 0.5 to 80 mils. Each model was run at a series of freestream Reynolds numbers, usually at a nominally constant stagnation temperature. The PANT series was run at $M_\infty = 5$ and the ART series was run mainly at $M_\infty = 8$.

Because of the large quantity of raw data it is necessary to condense it considerably. The test results that are probably of most interest are the heat-transfer rates at the beginning of the run when the wall is nearly isothermal.

Generally speaking surface roughness effects depend upon some Reynolds number parameter so that to observe them for small roughness heights a large freestream Reynolds number per foot is necessary. The capability of the NOL facility is high enough that the roughness influence upon heat transfer can be observed with models of moderately small roughness and above. The influence of roughness is to increase the heat-transfer rate when the height is above a critical value and to have no effect below that value. The purpose of these tests was to experimentally delineate the critical height and the dependence of heat transfer upon roughness height, freestream Reynolds number and body location.

In addition to the direct effect of surface roughness upon the boundary layer there is an indirect influence through the shift in the transition location. The tests reported herein have a sufficient range of Reynolds number that for all but the smoothest, transition could be brought onto the hemispherical nose.

Reports analyzing the test results in terms of contemporary knowledge of the influence of roughness on transition and heat transfer will be published as soon as each phase of the analysis is complete.

TEST APPARATUS

Test Conditions

The tests were conducted in the NOL Hypersonic Tunnel which is an intermittent, blowdown-type tunnel designed to operate at Mach numbers of 5 to 10. The tunnel utilizes an air supply system consisting of a 42,000-pound capacity, 5000-psia maximum pressure storage field and a combined pebble-bed, electric-resistance heater of 1500°F maximum temperature capability. A line diagram of the Hypersonic Tunnel is shown on Figure 1 and a detailed description of its performance capability may be found in Reference 1.

The present tests were conducted at Mach 5 and 8 at Reynolds numbers ranging from 2×10^6 to 21×10^6 per foot at Mach 5 and from 0.44×10^6 to 10×10^6 per foot at Mach 8. The conditions for each test run are given in Table 1.

Model Geometry and Instrumentation

The models were the same as used at NOL in the Passive Nosetip Technology program. The ART program included seven models of sphere-cone configuration of 2.5-inch nose radius (Models 2 to 8) and one model of blunted-cone configuration of 5-inch nose radius (Model 9). The cone half-angle of all models was 8°. The models were made of nickel (electroformed) and had a nominal wall thickness of 0.08 inch. The surface roughness ranged from 0.5 to 80 mils in height and were produced by either sandblasting or by brazing spherical copper particles. Each model was instrumented with 75 chromel-alumel thermocouples spot-welded to the inner surface. Model geometries and thermocouple arrangements are shown in Figure 2. Photographs of a sphere-cone model of 80-mil roughness and of the blunted-cone model are shown in Figure 3.

Thermocouple outputs were recorded with the Hypersonic Tunnel analog-to-digital recording system. The recording matrix was arranged to permit thermocouples near the stagnation point (fast-rising temperatures) to be recorded at twice the rate (every 0.28 second) of the thermocouples mounted on the frustum. Schlieren photographs, at a rate of two or more per run, were also taken.

Test Procedure

Before a test run the model was contained in a special enclosure permitting the model to be preheated or precooled uniformly to a prescribed temperature. During a test run the model was injected into the test stream, traversing the test jet boundary at a velocity of about 3 feet per second. The length of exposure varied from 8 to 80 seconds depending on the test condition. Specific values for each test run may be found in Table 1.

DATA REDUCTION AND PRESENTATION

Form of the Available Data

Typical examples of the time-temperature plots that are derived from the recorded thermocouple (TC) outputs are shown on Figure 4. The electrical output of the TC was recorded on magnetic tape during the tunnel run. Subsequently it was processed through a computer that uses known calibration constants to convert the electrical output to temperature. The computer produces a tape which automatically plots the time-temperature data as shown in Figure 4. These plots are useful to determine (1) the shape of the curve (straight or not), (2) the consistency of the data and (3) the slope obtained graphically. Because of the large number of data points and the difficulty of obtaining the slope accurately by graphical means, these plots were not used for the determination of the heat-transfer rate. The data-reduction process that was used is described below.

Each TC record allows the determination of (1) the initial wall temperature at that location, (2) the time at which the trace starts to depart from the baseline and (3) the initial slope of the time-temperature record from which the heat-transfer rate is determined by standard calorimeter methods. Although the thermal conduction along the model wall is not necessarily negligible, no correction has been applied for this effect.

Treatment of the Data

From a listing of temperature versus time for all TC's on a particular run, a nominal start time is established for each run. Before this time all outputs are seen to be nearly constant. This is the nominal beginning of the run. The actual time at which each TC will begin to rise need not be the same due to the fact that model injection is not instantaneous. Some TC's "feel the flow" before others.

The data reduction was performed by playing the data tape into a computer that was programmed to follow the procedure given below.

Based upon the nominal prerun portion of the output, an initial wall temperature, T_i, is obtained for each TC by averaging the prerun points. In the analysis of the data all points after the beginning of the run are ignored until the TC temperature has increased by 2°F above the prerun average. This increase is small enough to be just outside the normal scatter but large enough to eliminate any small "toe" that the data might have. The data taken after the 2°F rise was curve-fitted by a least squares technique. The curve was projected back to the known initial temperature to find the start time for that TC which is its own effective beginning of the run. The mean square deviation of the data points from the fitted curve (for those points used to establish the curve) was calculated in each case to give a measure of how well the curve

actually fits the data. Finally the initial slope of the curve was determined at the initial time, t_i. From the slope, the heat-transfer rate was computed knowing the wall thickness and the other properties of the wall material.

Curve Fitting the Time Temperature Data

Since the shape and character of the TC's time-temperature curve varies considerably depending upon its position on the body and the particular wind tunnel conditions, no single type of curve fit would be universally satisfactory. This is illustrated, to some extent, by the two curves in Figure 4. The data plots range from highly curved traces with few points to nearly straight traces in which the temperature is rising slowly and the noise (or least count) of the system is evident. Consequently the data from each TC was fitted by four different schemes. When the results were examined, it was possible to establish fairly accurately the initial slope. The consistency of the initial time with that of the other TC, the mean square deviation of the points from the curve and the inspection of the shape of the time-temperature plots (like those in Figure 4) were used to determine which form of curve fit is most likely to give the most accurate result.

After some experimentation with different order polynomials and different numbers of points, the following set of four was chosen as being a good basis upon which to proceed.

(1) A parabola based on three points. This is not a curve fit in the statistical sense because it passes through the first three data points exactly. It is useful for cases in which a large number of points cannot be used. For example, there are times when there is a sharp break or rapid change in slope early in the curve (like that in Figure 4b) which would not be approximated very well by any of the other curve fits.

(2) A third order polynomial fitted through the first six data points. This is a good approximation for highly curved traces with widely spaced points.

(3) A parabola fitted through eight points. This is widely applicable to well behaved traces.

(4) A straight line through 10 points. This is used with the nearly straight traces which are often found on the skirt of the body where the temperature rise is slower.

These curves have sufficient diversity and yet sufficient overlap that with reasonable confidence a value of slope can be determined from one of the methods in this set of four.

Data Derived From The Fitted Curve

Since the most appropriate curve fit is not known beforehand, the computer is programed to produce results for all four methods so that the most suitable can be selected afterwards. For the purpose of a preliminary reduction of the data, the stagnation heat rate was arbitrarily calculated on the basis of the cubic six point curve fit. The two TC's that are at the nose were averaged and the result was printed on the output as $\dot{q}_o$ in BTU/ft^{2}sec. All the data for the other TC locations is calculated as the ratio $\dot{q}/\dot{q}_o$. Each TC location has four values of $\dot{q}/\dot{q}_o$ and the corresponding mean square error which are calculated from the four curve fits.

After the data have been reduced to the preliminary form described above it is necessary to go through it and select the values that best represent the original data. This can usually be done on the basis of the form of the temperature-time curves and from the mean square error that is calculated for each of the curves (usually the mean square error was much less than 1°F). For the stagnation TC a tabulation of the temperature history together with the corresponding fitted points is printed out. From these tables it is possible to distinguish between systematic differences and random errors in the few cases in which the choice of curve fitting methods is not already clear. The most probable value of $\dot{q}_o$ as determined by the above procedure is given in Table 1 together with the run conditions.

The data for the other TC locations were handled in a fashion similar to that for the stagnation point. The most representative curve fit was chosen on the basis of the shape of the temperature-time plots as well as the smallness of the mean square deviation from the fitting curve. The value of $\dot{q}/\dot{q}_o$ was adjusted to allow for the fact that the most accurate value of $\dot{q}_o$ was not always that obtained from the cubic curve fit. In order to compress the data the heat transfer was averaged on rings (all runs were at zero degree angle of attack). The heat-transfer distributions are given in Table 2. The value of $\dot{q}_o$ that is used to nondimensionalize them is the value given in Table 1.

At TC locations away from the nose (usually on the skirt) the temperature-time curve might suffer a sudden change in slope such as that shown in Figure 4b. This undoubtedly is due to transition shifting across the TC during the run. For cases in which this happens the initial slope is marked (L) or (H) in Table 2 to indicate that it is the lower or higher of the two slopes. In some cases the slope change is too near the beginning of the run to accurately measure the initial heating rate. In those cases the data were omitted and a blank is left in Table 2.

SYMBOLS

H	refers to the higher temperature-time slope value when there is an abrupt change
k	wall roughness element height, mils
L	refers to the lower temperature-time slope value when there is an abrupt change
M_∞	free-stream Mach number
P_o	air supply pressure, psia
$\dot{q}$	heating rate, BTU/ft^2-sec
$\dot{q}_i$	initial heating rate, BTU/ft^2-sec
$\dot{q}_o$	stagnation point heating rate, BTU/ft^2-sec
R	radius, in.
$R_{e\infty}$	free-stream Reynolds number
R_n	nose radius, in.
S	distance along model surface, in.
t_i	initial time, sec
T_i	initial wall temperature, deg F
T_o	air supply temperature, deg F
TC	thermocouple
X	axial distance from the stagnation point, in.
ϕ	azimuth angle from the model top, deg

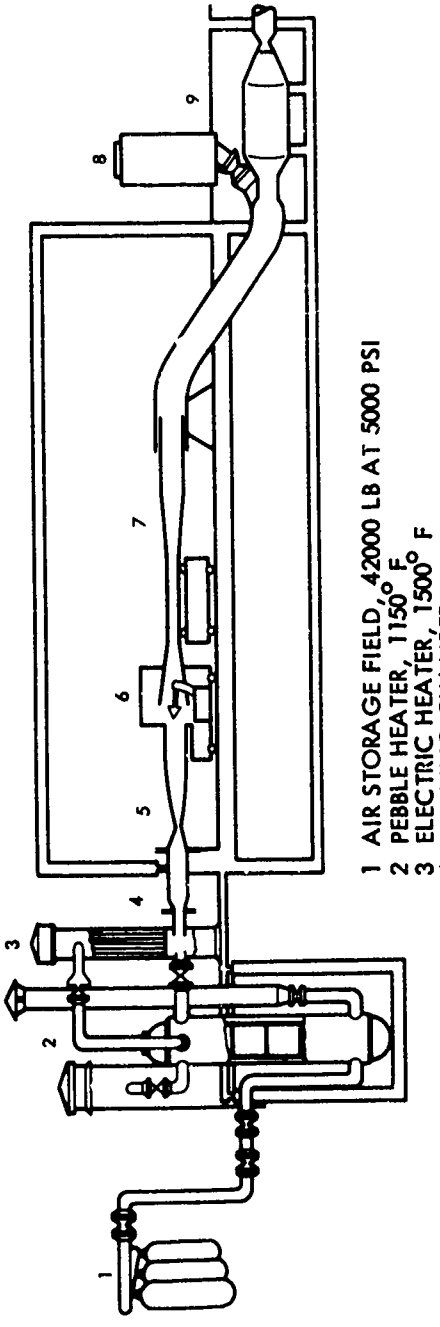

FIG. 1 NOL HYPERSONIC TUNNEL

SURF. DIST.	SURF. DIST.	AXIAL LOCAT.	CIRCUMFERENTIAL LOCATION, ϕ, DEG							
S/R_N	S/R_N DEG	X IN	0	45	90	135	180	225	270	315
.0	0°		1							75
.209	12°		2		3		4		5	
.419	24°		6		7		8			
.628	36°		9	10	11		12	13	14	15
.838	48°		16		17		18			
1.047	60°		19		20		21	22	23	24
1.257	72°		25	26	27	28	29			
1.431	82°		30				31	32	33	34
1.591		2.5	35	36	37	38	39			
1.791		3.0	40				41	42	43	44
2.190		4.0	45	46	47	48	49			
2.589		5.0	50				41	52	53	54
3.188		6.5	55			56	57			
3.787		8.0	58	59	60		61	62	63	64
4.186		9.0				66	67			
4.585		10.0	68	69	70		71	72	73	74

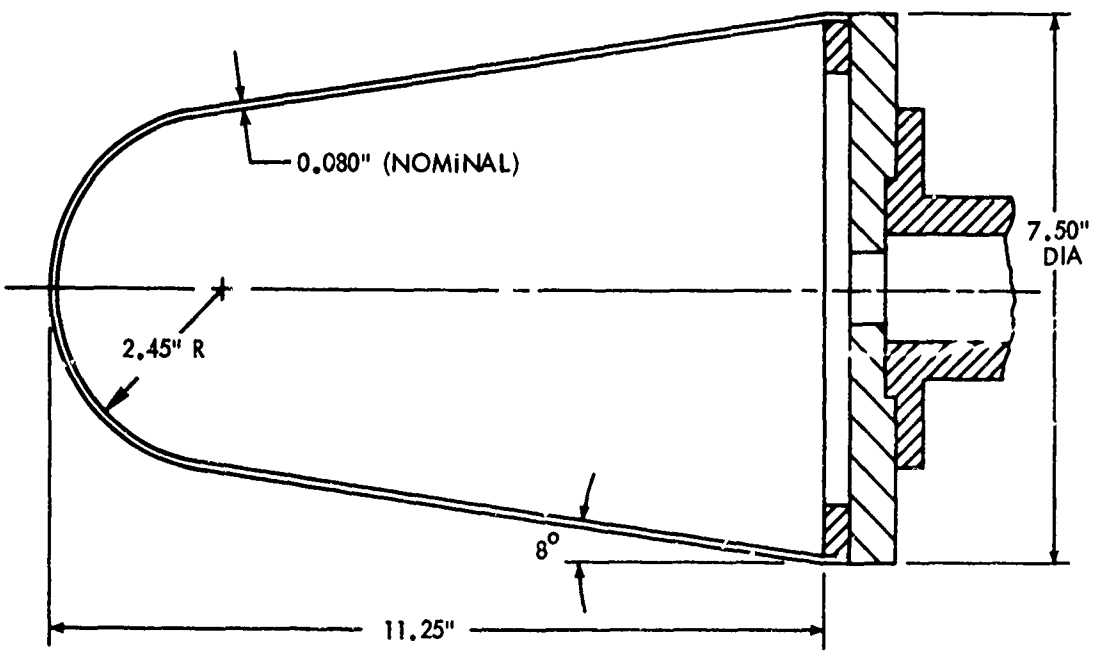

A. SPHERE-CONE CONFIGURATION

FIG. 2 MODEL GEOMETRY AND INSTRUMENTATION LAYOUT

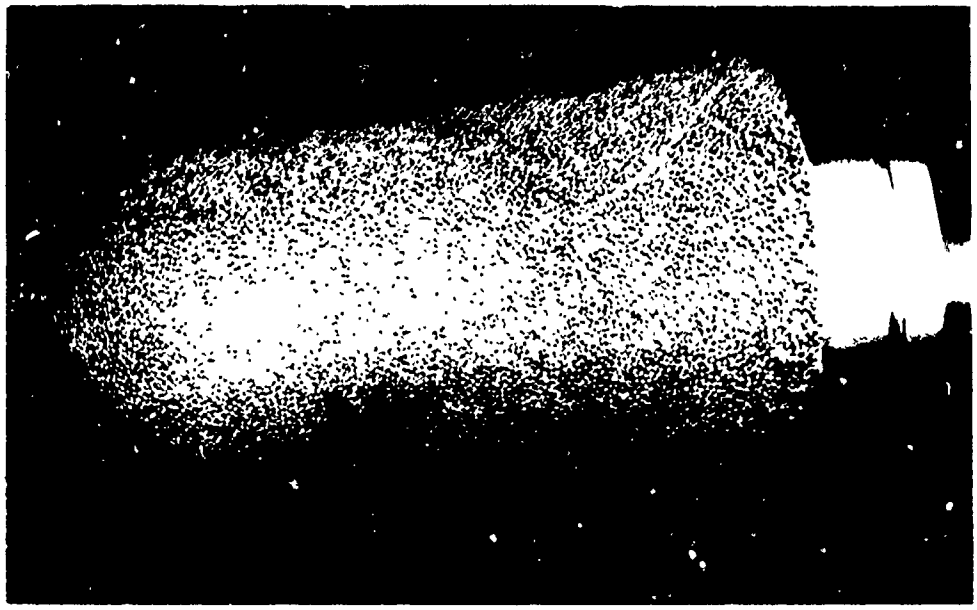

A. SPHERE-CONE WITH 80-MIL ROUGHNESS (MODEL NO. 8)

B. BLUNTED-CONE WITH 3-MIL ROUGHNESS (MODEL NO. 9)

FIG. 3 MODEL PHOTOGRAPHS

S/R_n*	SURF. DIST. S IN	AXIAL LOCAT. X IN	CIRCUMFERENTIAL LOCATION, ϕ, DEG							
			0	45	90	135	180	225	270	315
0	0	0	1							74
.20	.50		2		3		4		5	
.40	1.00		6				7			
.60	1.50		8	9	10	11	12	13	14	15
.80	2.00		16				17			
1.00	2.50		18	19	20	21	22	23	24	25
1.16		1.00	26	27	28	29	30			
1.36		1.50	31	32	33	34	35			
1.56		2.00	36		37		38		39	
1.77		2.50	40				41			
1.91		3.00	42	43	44	45	46	47	48	49
2.17		3.50	50				51			
2.57		4.50	52		53		54		55	
2.98		5.50	56				57			
3.39		6.50	58	59	60	61	62	63	64	65
4.00		8.00	66		67		68		69	
4.62		9.50	70		71		72		73	

*BASED ON R_N = 2.5 IN

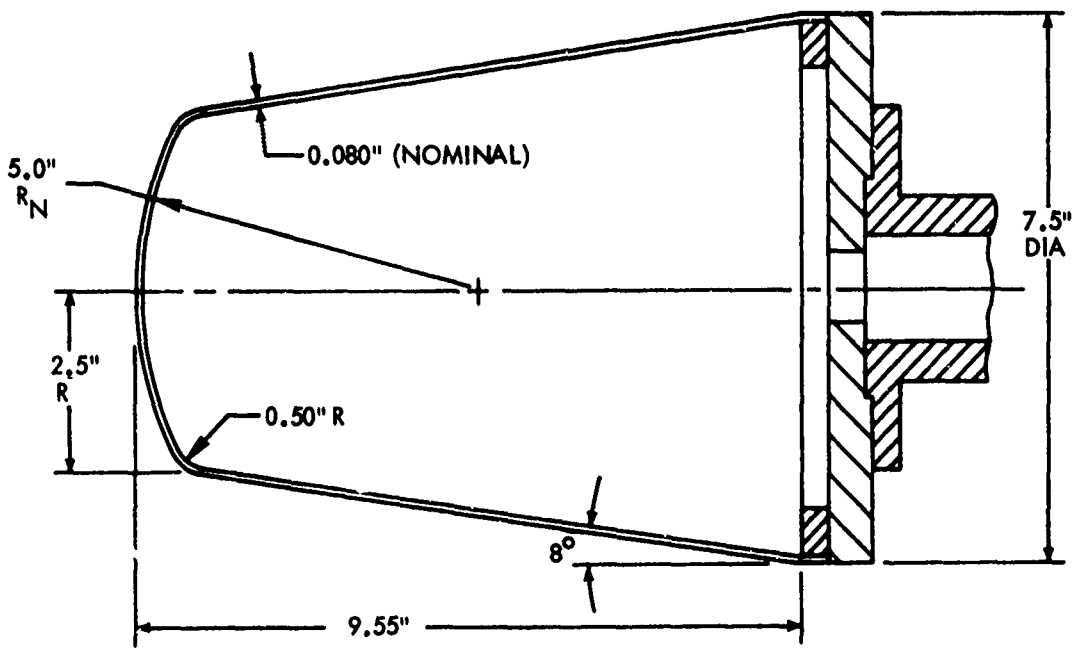

8. BLUNTED-CONE CONFIGURATION

FIG. 3 (CONTINUED)

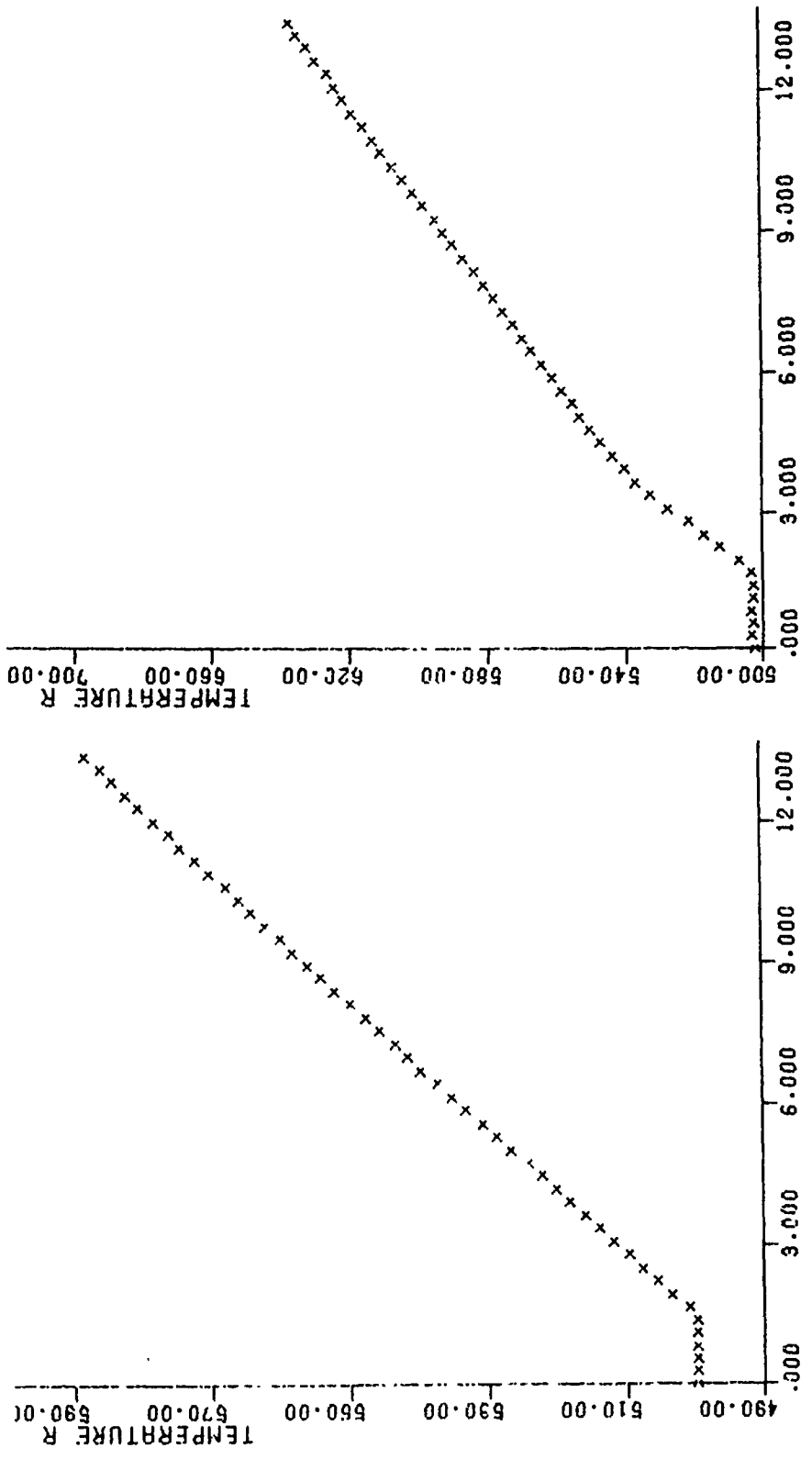

FIG. 4 SAMPLES OF TEMPERATURE-TIME TRACES

Table 1

TEST CONDITIONS AND STAGNATION POINT INITIAL HEATING RATE

Run	Model No.	Model k mils	Free-Stream M_∞	Free-Stream Re_∞ 10^6 Ft^{-1}	Air Supply P_o psia	Air Supply T_o °F	Initial Temp. T_i, °F	Stag. Pt. Initial Heating BTU/Ft^2/sec	Exposure Time sec
2	9	3	5.00	20.95	82.75	1192	501	24.3	8.5
3	9	3	5.00	7.306	28.30	1177	511	13.1	12
4	9	3	4.98	4.79	18.03	1161.5	525	8.49	14
5	9	3	4.97	3.16	11.75	1157	509	8.01	16
6	9	3	4.97	1.935	7.185	1155	520	5.42	18
7	9	3	7.90	8.50	134.6	1432	524	17.65	13
8	9	3	7.91	7.07	111	1423	513	16.0	14
9	9	3	7.90	5.36	82	1402	510	12.4	17
10	9	3	7.84	3.60	52.9	1385	512	9.5	19
11	9	3	7.79	1.92	26.7	1350	520	6.3	21
12	7	40	7.73	10.21	151.3	1420	530	42.0	13
13	7	40	7.86	4.19	63.3	1401.5	516	25.9	21
14	7	40	7.79	1.92	26.6	1348	517	12.2	32
15	7	40	7.75	1.07	14.55	1339	507	7.59	37
16	7	40	7.72	.536	6.99	1316	499	5.37	60
17	7	40	7.70	.368	4.28	1235	503.5	2.89	80
18	7	40	7.73	.866	11.61	1336	496.5	6.70	50
19	5	3	7.90	9.13	148.4	1455	512	24.8	13
20	5	3	7.91	6.835	109.1	1437	527	19.6	16
21	5	3	7.90	5.25	82.1	1421	509	17.2	18
22	5	3	7.85	3.76	57.9	1421	504	13.8	21
23	5	3	7.82	2.96	43.9	1396	514	11.3	25
24	5	3	7.87	2.27	33.6	1380	518	7.59	28
25	5	3	7.78	1.67	23.6	1366	517	7.71	32
26	6	10	7.90	8.98	148.5	1470	514	36.4	13
27	6	10	7.90	5.18	82.4	1435	530	21.2	18
28	6	10	7.84	3.58	54.9	1420	496	15.7	21
29	6	10	7.81	2.45	36.35	1396	504	12.0	27
30	6	10	7.79	1.78	25.5	1375	524	9.39	33
31	6	10	7.75	1.32	18.35	1361	510	7.81	40
32	6	10	7.74	.932	12.71	1348	511	5.79	50
33	8	80	7.77	1.974	20.37	1135	514	9.51	36
34	8	80	7.75	1.467	14.99	1132	502	8.08	40
35	8	80	7.74	1.082	11.02	1131	498	6.47	50
36	8	80	7.72	.819	8.32	1135	497	5.12	55
37	8	80	7.70	.597	5.87	1118	511	3.60	65

Table 1 (Cont.)

Run	Model No.	Model k mils	Free-Stream M_∞	Free-Stream Re_∞ 10^6 Ft^{-1}	Air Supply P_o psia	Air Supply T_o °F	Initial Temp. T_i, °F	Stag. Pt. Initial Heating $BTU/Ft^2/sec$	Exposure Time sec
38	8	80	7.90	9.49	149.55	1428	489	37.1	13
39	8	80	7.90	5.15	82.12	1437.5	485.5	43.4	18
40	8	80	7.83	3.12	47.73	1420	488.5	27.9	23
41	8	80	7.80	2.086	30.87	1400	486	20.1	30
42	8	80	7.77	1.435	20.51	1380	489	16.1	36
43	8	80	7.75	1.07	14.87	1362	486	9.79	40
44	8	80	7.73	.80	11.17	1369	400.5	9.24	50
45	8	80	7.72	.611	8.30	1350	505	6.78	55
46	8	80	.70	.440	5.87	1341	503	4.90	65
47	3	1.5	7.90	8.80	149.2	1492	484	23.9	13
48	3	1.5	7.91	6.62	109.5	1468	482	17.6	15
49	3	1.5	7.90	7.85	129.3	1466	487	19.9	13
50	3	1.5	7.90	5.20	81.5	1423	488.5	14.5	18
51	3	1.5	7.74	.968	13.24	1350	500.5	5.11	20
52	3	1.5	7.91	6.94	111.4	1442	605	13.9	15
53	3	1.5	7.86	4.12	62.0	1400	498	12.0	22
54	4	3	7.90	9.04	148.6	1465	478	22.5	13
55	4	3	7.90	7.80	116.1	1463	494	20.0	15
56	4	3	7.90	5.50	88.5	1446	503	16.2	20
57	4	3	7.90	4.73	75.17	1435	503	14.5	21
58	4	3	7.86	4.02	62.4	1425	504	12.9	22
59	4	3	7.83	3.34	51.4	1424	511	12.0	23
60	4	3	7.90	5.54	89.5	1450	641	11.9	15
61	2	0.5	7.90	8.86	148.7	1483	535	20.5	10
62	2	0.5	7.90	7.97	135.1	1492	533	20.5	10
63	2	0.5	7.90	8.65	142.3	1466	535	20.0	10
64	2	0.5	7.90	8.18	134.5	1465	535	19.7	10
65	2	0.5	7.90	7.86	127.5	1453	540	18.7	10

Table 2

MODEL WALL TO STAGNATION POINT INITIAL HEATING RATES

Thermoc. Location S/R	Model 2, k = .05 mil Run 61	62	63	64	65
0	1.000	1.000	1.000	1.000	1.000
.21	.875	.871	.871	.892	.862
.42	.863	.841	.862	.845	.846
.63	.746	.704	.731	.707	.700
.84	.571	.535	.545	.515	.514
1.05	.412	.334	.356	.331	.321
1.26	.234	.217	.236	.214	.214
1.43	.160 L	.123	.134	.122	.144
1.59	.123 L	.094	.115	.090	.113
1.79	.130	.083	.088	.083	.082
2.19	.166 H	.074	.164 H	.075	.071
			.076 L		
2.59	.195 H	.133 H	.182 H	.068	.064
		.067 L	.070 L		
3.19	.200 H	.128 H	.185 H	.108 H	.158 H
		.060 L		.056 L	.059 L
3.79	.182 H	.214 H	.184	.168 H	.128 H
		.054 L		.053 L	.052 L
4.19	.227 H	.146 H	.188	.140 H	.133 H
		.056 L		.051 L	.041 L
4.59	.229 H	.120 H	.181	.177 H	.115 H
		.053 L		.055 L	.045 L

H High slope
L Low slope

Thermoc. Location S/R	Model 3, k = 1.5 mils Run 47	48	49	50	51	52	53
0	1.000	1.000	1.000	1.000	1.000	1.000	1.000
.21	1.036	.984	.999	1.016	.995	1.034	1.029
.42	1.131	.940	.963	.881	.860	.911	.877
.63	1.603 H	.958	1.419	.744	.739	.783	.733
.84	1.251 H	1.094	1.276	.516	.539	.628	.490
1.05	.799 H	.743 H	.797 H	.341	.365	.409	.337
1.26	.421 H	.307 H	.424 H	.214	.230	.198	.195
1.43	.207 H	.158 H	.211 H	.133	.140	.133	.129
1.59	.206 H	.109 H	.186 H	.108	.110	.107	.106
1.79	.268 H	.200 H	.272 H	.087	.088	.091	.086
2.19	.249 H	.238 H	.201 H	.077	.077	.082	.075
2.59	.214 H	.280 H	.162 H	.069	.071	.077 L	.069
3.19	.192 H	.311 H	.162 H	.062	-	.075 L	.055
3.79	.162 H	.234 H	.144 H	.051	.048	.067 L	.045
4.19	.169 H	.246 H	.195 H	.049	.053	.063 L	.048
4.59	.161 H	.222 H	.170 H	.046	.049	.062 L	.044

Table 2 (Continued)

Thermoc. Location S/R	Model 4, k = 3 mils (sand blasted) Run 54	55	56	57	58	59	60
0	1.000	1.000	1.000	1.000	1.000	1.000	1.000
.21	1.352	1.132	1.048	1.012	1.018	.980	1.053
.42	1.959	1.681	1.357	1.094	.951	.859	1.198
.63	2.036	1.785	1.363	1.452	1.135	.833	1.603
.84	1.701	1.489	1.353	1.246	1.148	.752	1.358
1.05	1.237	1.062	.970	.872	.788 H	.529	.932
1.26	.730	.615	.543	.48	.426 H	.247	.509
1.43	.366	.304 H	.269	.238 H	.198	.150	.204
1.59	.287	.232 H	.188	.161	.138	.077	.136
1.79	.260	.224	.209 H	.135 H	.101	.083	.219 H
2.19	.241	.213	.214 H	.196 H	.081	.069	.254 H
2.59	.223	.197	.191 H	.210 H	.135 H	.062	.258 H
3.19	.204	.181	.178 H	.176 H	.117 H	.056	.214 H
3.79	.184	.164	.162 H	.156 H	.123 H	.049	.200 H
4.19	.177	.157	.157	.158 H	.155 H	.048	.199
4.59	.162	.146	.143 H	.141 H	.150 H	.043	.190 H

Thermoc. Location S/R	Model 5, k = 3 mils (Braised particles) Run 19	20	21	22	23	24	25
0	1.000	1.000	1.000	1.000	1.000	1.000	1.000
.21	1.340	1.080	.943	.952	.927	.946	.935
.42	2.036	1.805	1.220	.862	.774	.850	.782
.63	2.001	1.886	1.707 H	1.005	.626	.681	.641
.84	1.596	1.472	1.299 H	.998	.471	.475	.485
1.05	1.034	.910	.778 H	.565	.321	.328	.339
1.26	.516	.416	.352 H	.302	.203	.204	.215
1.43	.270	.253	.204 H	.141	.142	.140 L	.148 L
1.59	.235	.190	.151 H	.107	.1[illegible]	.109 L	.111 L
1.79	.215	.188 H	.151 H	.075	.081	.083	.082 L
2.19	.206	.194 H	.205 H	.071	.073	.073	.075
2.59	.189	.179	.183	.062	.067	.067	.067
3.19	.172	.163	.151	.057	.059	.059	.059
3.79	.159	.153	.143	.153 H	.054	.053	.055
4.19	.145	.141	.131	.130 H	.048	.048	.050
4.59	.140	.137	.127	.122 H	.046	.047	.047

Table 2 (Continued)

Thermoc. Location S/R	Model 6, k = 10 mils Run 26	27	28	29	30	31	32
0	1.000	1.000	1.000	1.000	1.000	1.000	1.000
.21	1.238	1.087	.996	.959	.840	.818	.818
.42	1.626	1.552	1.529	1.306	.885	.754	.722
.63	1.414	1.465	1.435	1.281	1.020	.633	.600
.84	1.147	1.163	1.183	1.042	.851	.478	.453
1.05	.767	.727	.734	.608	.444	.290	.282
1.26	.414 H	.385	.353 H	.292 H	.221	.165	.174
1.43	.269 H	.229	.234 H	.183 L	.141 H	.116	.125
1.59	.212	.168	.160	.114 L	.091 L	.084 L	.093 L
1.79	.178	.156	.132	.084 L	.067 L	.064 L	.072 L
2.19	.165	.147	.142	.102 H	.055	.060	.066
2.59	.153	.135	.132	.104 H	.049	.053	.059
3.19	.136	.122	.121	.114 H	.038	.045	.051
3.79	.119	.108	.108	.104 H	.037	.039	.046
4.19	.112	.103	.102	.095 H	.034	.039	.043
4.59	.099	.094	.095	.088	.032	.036	.040

Thermoc. Location S/R	Model 7, k = 40 mils Run 12	13	14	15	16	17	18
0	1.000	1.000	1.000	1.000	1.000	1.000	1.000
.21	1.473	1.191	1.030	1.047	.951	.980	.964
.42	1.931	1.433	1.241	1.151	.804	.929	.942
.63	1.726	1.327	1.181	1.101	.686	.760	.863
.84	1.256	.996	.892	.777	.480	.535	.684
1.05	.800	.623	.533	.466	.281	.336	.421
1.26	.462 H	.333 H	.293	.248 H	.164	.212 L	.218 H
1.43	.265	.214	.173	.077 L	.104	.146 L	.126 L
1.59	.209 L	.166 L	.123	.096 L	.087	.118 L	.090 L
1.79	.172 L	.125 L	.086 L	.058 L	.058	.086 L	.057 L
2.19	.164	.121	.085	.051 L	.050 L	.071 L	.045 L
2.59	.164	.120	.093	.047	.053	.071	.046 L
3.19	.150	.108	.087	.044	.045	.061	.039
3.79	.134	.097	.0805	.038	.040	.053	.035
4.19	.129	.091	.077	.040	.041	.048	.035
4.59	.121	.085	.073	.033	.035	.048	.031

Table 2 (Continued)

Thermoc. Location S/R	Model 8, k = 80 mils (Cold flow) Run 33	34	35	36	37
0	1.000	1.000	1.000	1.000	1.000
.21	1.136	1.011	1.025	1.008	.973
.42	1.228	1.044	1.109	.974	.923
.63	1.132	1.052	1.006	.868	.775
.84	.811	.771	.780	.691	.583
1.05	.515	.476	.442	.427	.336
1.26	.298	.271	.242	.236	.193 L
1.43	.178	.159 L	.143 L	.134	.121 L
1.59	.130	.104 L	.091 L	.086 L	.082 L
1.79	.195	.078 L	.057 L	.051 L	.065 L
2.19	.089	.073 L	.050 L	.041 L	.047 L
2.59	.087	.068	.044	.042	.038 L
3.19	-	-	-	-	-
3.79	.072	.059	-	-	-
4.19	.068	.062	.041	.030	.036
4.59	.065	.059	.041	.029	.0315

Table 2 (Continued)

Thermoc. Location S/R	Model 8, k = 80 mils Run 38	39	40	41	42	43	44	45	46
0	1.000	1.000	1.000	1.000	1.000	1.000	1.000	1.000	1.000
.21	2.095	1.253	1.163	1.173	1.052	1.182	.984	.974	.985
.42	2.448	1.334	1.261	1.301	1.111	1.271	.964	.935	.927
.63	2.181	1.225	1.182	1.210	1.047	1.171	.874	.817	.770
.84	1.799	.982	.951	.954	.812	.929	.712	.653	.581
1.05	1.153	.608	.564	.541	.462	.538	.432	.394	.343
1.26	.669	.356	.326	.322	.268	.305	.236	.217	.191 L
1.43	.413	.202	.209	.201	.161 L	.175 L	.135	.127 L	.116 L
1.59	.319	.146	.152	.144	.104 L	.125 L	.092	.061 L	.080 L
1.79	.272	.127	.130	.116	.084 L	.094 L	.062	-	.062 L
2.19	.236	.128	.115	.107	.080 L	.075	.049	.046 L	.046 L
2.59	.222	.119	.107	.101	.076	.074	.044	.037 L	.044 L
3.19	.203	.108	.099	.093	.071	.074	.044	.035	-
3.79	.182	.097	.089	.088	.065	.072	.047	-	-
4.19	.173	.092	.082	.074	.061	.068	.034	.030	.033
4.59	.159	.084	.075	.066	.055	.063	.036	.028	.034

Table 2 (Continued)

Thermoc. Location S/R	Model 9, k = 3 mils (Blunt, M_∞ = 5) Run 2	3	4	5	6	7	8	9	10	11
0	1.000	1.000	1.000	1.000	1.000	1.000	1.000	1.000	1.000	1.000
.2	1.917	1.080	1.070	.956	.980	.946	.908	.936	.956	.964
.4	3.215	2.062	1.572	.980	.997	1.286	1.103	.985	.967	.919
.6	3.704	2.644	2.549	1.424	1.205	1.856	1.736	1.179	.938	.891
.8	4.222	3.070	3.033	2.314	1.434	2.210	2.146	1.997	1.081	.905
1.0	2.927	2.034	1.972	1.462	.932	1.368	1.268	1.160	.715	.588
1.16	.769	.653 H	.700 H	.379 H	.331 H	.351 H	.418	.387 H	.286 H	.239 L
1.36	.685	.462 H	.358 L	.099 L	.171 L	.148 L	.094 L	.124 L	.090 L	.105 L
1.56	.790	.541	.458 H	.148 L	.217 H	.283 H	.132 L	.124 L	.119 L	.128 L
1.77	.817	.565	.554 H	.137 H	.262 H	.311	-	.112	.109 L	.118
1.91	.865	.584 H	.544 H	.145 L	.257 H	.314	.356 H	.108	.105	.112
2.17	.824	.573	.527	.143 H	.249 H	.368	.366 H	.099	.099	.110
2.57	.800	.514 H	.481	.332 H	.227	.295	-	.090	.090	.094
2.98	.748	.487	.449	.467	.212	.274	.218 H	.083	.083	.089
3.39	.692	.448	.413	.415 H	.195	.245	.245 H	.077	.074	.078
4.00	.609	.386	.368	.320 H	.174	.213	.195 H	.070	.064	.066
4.62	.594	.366	.361	.308 H	.171	.210	.191 H	.066	.062	.065